Journal of Applied Polymer Science

Synthesis and properties of click coupled graphene oxide sheets with three-dimensional macromolecules

Sibdas Singha Mahapatra, Madeshwaran Sekkarapatti Ramasamy, Hye Jin Yoo, Dong Hun Yi, Jae Whan Cho

Department of Organic and Nano System Engineering, Konkuk University, Seoul 143-701, Korea

Correspondence to: J. W. Cho (E-mail: jwcho@konkuk.ac.kr)

ABSTRACT: A facile click chemistry approach to the functionalization of three-dimensional hyperbranched polyurethane (HPU) to graphene oxide (GO) nanosheets is presented. HPU-functionalized GO samples of various compositions were synthesized by reacting alkyne-functionalized HPU with azide-functionalized GO sheets. The morphological characterization of the HPU-functionalized GO was performed using transmission electron microscopy and its chemical characterization was carried out using Fourier transform-infrared spectroscopy, nuclear magnetic resonance spectroscopy, and X-ray photoelectron spectroscopy. The graphene sheet surfaces were highly functionalized, leading to improved solubility in organic solvents, and consequently, enhanced mechanical, thermal, and thermoresponsive and photothermal shape memory properties. The strategy reported herein provides a very efficient method for regulating composite properties and producing high performance materials. © 2016 Wiley Periodicals, Inc. J. Appl. Polym. Sci. **2016**, *133*, 43358.

KEYWORDS: click chemistry; composites; graphene; nanotubes; polyurethanes

Received 2 September 2015; accepted 17 December 2015

DOI: 10.1002/app.43358

INTRODUCTION

Shape-memory materials are a class of smart materials that respond to external stimuli, typically temperature and their applications have expanded steadily as well as academic and industry. Shape-memory polymers (SMP) have received more attention owing to their low cost, low density, easy processability compared with shape-memory alloys, ceramics, hydrogels, etc.[1,2] However, SMPs suffer from relatively weak recovery force due to their low stiffness when compared with most other shape memory alloys. To overcome this problem, SMP nanocomposites have been proposed where an SMP matrix is reinforced with nanomaterials with a high aspect ratio.[3–6]

Among the nanomaterials graphene is a novel allotrope of carbon consisting of two-dimensional layers of sp^2-bonded atoms, and has drawn tremendous attention because of its extraordinary properties such as its high Young's modulus, thermal and electrical conductivity, mobility of charge carriers among others.[7–10] The uniform dispersion of graphene oxide (GO), a modified and promising form of graphene, in polymer hosts and the favorable interfacial interactions between the two resulting phases are crucial for the successful development of high-performance composites.[11–15] Until now, homogeneous graphene sheet dispersions have been prepared using both covalent and non-covalent functionalization. Generally, chemical hybridization on the nanoscale is superior to physical blending on the macroscale due to the well dispersion and improved interface between polymer and filler in the former case. Covalently incorporated fillers provide multifunctional crosslinks that enhance the rubber elasticity and strain recovery of a shape memory material.[16,17]

On the other hand, hyperbranched polymers are highly branched macromolecules with three-dimensional dendritic architectures, and have become very popular because of their low viscosity, good solubility, and potential for containing multiple functionalities.[18–21] In addition, one-pot, self-polymerized hyperbranched polymers are superior to dendrimers for large-scale production because they are easier to prepare. Furthermore, polymer properties can be tailored through monomer selection and functional group modification. Incorporating globular hyperbrached polymers into GO should significantly alter the intercalation process and may allow for the formation of individual GO nanosheets.[22]

However, general strategy for covalent functionalization of polymers onto graphene sheets undergoes from significant drawbacks. For example, direct coupling with surface-bound carboxylic acid, epoxy, or alcohol groups on GO sheets involves low efficiency and tedious processes.[23] Meanwhile, *in situ* polymerization with a graphene-functionalized initiator gives low yields and minimal control of molecular weight and architecture, necessitating precise reaction conditions.[24] Therefore, it is necessary to explore an alternative techniques for preparing

polymer-grafted graphene sheets with high efficiency and mild reaction conditions while providing good control over polymer structure and molecular weight.

Click chemistry, characterized by its modular nature, high selectivity, and excellent yields, has been significantly developed recently. The Cu-catalyzed Huisgen 1,3-dipolar cycloaddition between azides and alkynes plays a particularly important role and has received enormous attention in polymer and materials science since its reinvention in 2001.[25,26] Notably, it can proceed in the presence of all functional groups because of its high reactivity and reliability and is not affected by the presence of H_2O, O_2, etc. Since this technique has been successfully used to modify both carbon nanotubes (CNTs)[27–30] and fullerenes,[31] it would be quite efficient for the functionalization of GO, the analogue of CNTs.

In this study, we utilize azide-alkyne click chemistry to functionalize GO with hyperbranched polyurethane. HPU/GO nanocomposites with three different wt % of GO were prepared, and their potential as SMPs was investigated. The effect of GO on various properties such as the mechanical and thermal properties of the hyperbranched matrix was also reported.

EXPERIMENTAL

Materials

The GO used in this study was purchased from NanoInnova Technologies (Madrid, Spain). 4,4′-methylene *bis*(phenylisocyanate), triethanolamine, propargyl bromide, 2-chloroethyl isocyanate, sodium azide, copper bromide, and *N*,*N*,*N*′,*N*′,*N*″-pentamethyldiethylenetriamine (PMDETA) were purchased from Sigma-Aldrich and used without further purification. Poly(ε-caprolactone)diol (PCL, M_w: 3000 g/mol) was obtained from Solvay (UK).

Preparation of 2-Chloroethyl Isocyanate-Treated GO

2-Chloroethyl isocyanate-treated GO was synthesized as described in the literature.[32] In a typical procedure, 200 mg of GO was homogenously suspended in 15 mL of anhydrous *N*,*N*-dimethylformamide (DMF) by sonication for 15 min. This suspension was then loaded into a 50 mL round-bottom flask equipped with a magnetic stirring bar, to which 2 mL of 2-chloroethyl isocyanate was added while the mixture was stirred under nitrogen. After 24 h of stirring, the product was coagulated into by the addition of methylene chloride (50 mL). The product was then filtered through a 220 nm polytetrafluoroethylene membrane, washed with additional methylene chloride (50 mL), and dried under vacuum.

Preparation of Azide-Functionalized Graphene (GO-Azide)

To prepare azide-functionalized GO (GO-Azide), 200 mg of 2-chloroethyl isocyanate-treated GO was dissolved in 20 mL of DMF by sonication; 30 mmol of sodium azide powder was then added under sonication in an ice bath and left there for 30 min. The mixture was stirred and refluxed for 24 h at 70°C in an oil bath, introducing the azide group through nucleophile substitution at the alkyl halide. The product was then filtered through a 220 nm polytetrafluoroethylene membrane, washed with additional methanol (100 mL), and dried under vacuum.

Synthesis of Mono-Propargyl Pentaerythritol

Mono-propargyl pentaerythritol was synthesized as described in the literature.[33,34] Pentaerythritol (4 g, 29.4 mmol) and *p*-toluenesulfonic acid monohydrate (56 mg, 0.30 mmol) were combined in 40 mL of dry toluene and heated to reflux. Triethyl orthoacetate (5.4 mL, 29.4 mmol) was added to the flask, and the resulting suspension was refluxed for 96 h. The solution was filtered and concentrated under reduced pressure, yielding a white solid. The resulting orthoacetate protected product (0.80 g, 5.0 mmol) was then dissolved in anhydrous DMF (10 mL) and cooled to 0°C under nitrogen. Sodium hydride (0.20 g, 60 wt %, 5.0 mmol) was added to the cooled solution, which was stirred for 30 min; propargyl bromide was then added, followed by an additional 24 h of stirring. Finally, brine (120 mL) was added to the reaction mixture, which was extracted with ethyl acetate (120 mL); the organic phase was then dried.

The propargyl-functionalized product was redissolved in 50 mL of methanol; a catalytic amount of hydrochloric acid was then added, and the mixture was stirred at 40°C for 3 h. Next, the pH was increased with 0.1*N* NaOH solution before the solution was filtered, concentrated, and purified by silica gel chromatography. The mono-propargyl pentaerythritol product was obtained in three steps from pentaerythritol.

Synthesis of Alkyne-Containing HPU (HPU-Alkyne)

First, 8 g of PCL (2.66 mmol) was dissolved in 30 mL of dry DMF in a 500 mL three-necked cylindrical vessel equipped with a mechanical stirrer and nitrogen inlet. 2 g of 4,4′-methylene bis(phenylisocyanate) (8 mmol) dissolved in 10 mL of DMF was slowly added to the vessel at room temperature. The reaction temperature was slowly increased to 70°C and maintained at that temperature for 3 h for prepolymer synthesis. In the second step, the system was cooled to 0 to 5°C, and 0.448 g of mono-propargyl pentaerythritol (2.56 mmol) and 0.04 g of dibutyltin dilaurate dissolved in 10 mL DMF were added. The temperature was then increased slowly to 60°C, and the solution was left to react for 3 h. The final viscous product was dried in a hot air oven at 50°C for 48 h to obtain the polymer films.

Synthesis of Nanocomposites Using Click Chemistry

Coupling of the HPU-alkyne and GO-Azide was carried out via Cu(I)-catalyzed click chemistry. First, 20 mg of the GO-Azide was dispersed in 15 mL of DMF by sonication at room temperature for 10 min. The suspension was added to a two-necked flask equipped with a reflux condenser and magnetic stir bar containing 1 g of the HPU-alkyne in 15 mL of DMF; the resulting mixture yielded a homogenous solution shortly thereafter, which was deoxygenated by bubbling with nitrogen for 30 min. Next, 19.2 mg of copper bromide (0.134 mmol) and 28.2 μL of PMDETA (0.163 mmol) were added, after which the solution was heated to 60°C and continuously stirred under nitrogen atmosphere at this temperature for 24 h. The product was precipitated in water and, and then dried overnight under vacuum at room temperature. HPU-functionalized GO nanosheets with different compositions were synthesized by using 0.5, 1, or 2 wt

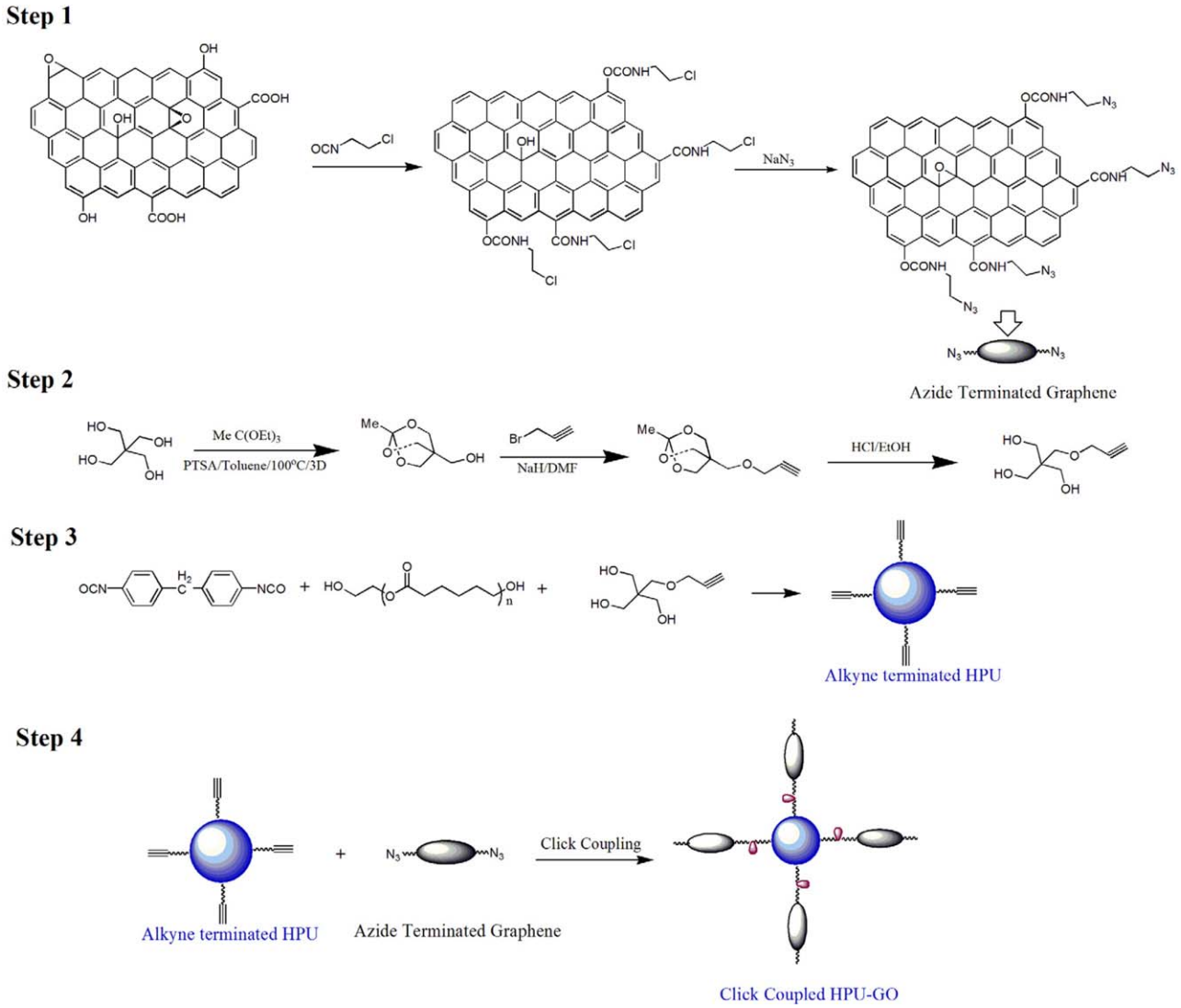

Scheme 1. Schematic representation of the synthesis of the graphene sheet grafted hyperbranched polymer by click chemistry approach. [Color figure can be viewed in the online issue, which is available at wileyonlinelibrary.com.]

% GO-Azide; the corresponding samples are denoted as GHPU(0.5), GHPU(1), and GHPU(2), respectively.

Measurements

Fourier transform-infrared (FT-IR) spectra of the polymer were recorded on a Jasco FT-IR 300E. ^{1}H NMR spectra of the samples were recorded with a Bruker 400-MHz NMR spectrometer using DMSO-d_6 as the solvent and tetramethylsilane as the internal standard. Differential scanning calorimetry (DSC) measurements were carried out using a TA Instruments 2010 thermal analyzer in a temperature range of −50 to 250°C, at a heating rate of 10°C min^{-1}, and under nitrogen flow. X-ray photoelectron spectroscopy (XPS, ESCSA 2000) was used to analyze the surface composition of the graphene sheets. The surface morphology of GO and HPU-functionalized GO was observed by high resolution transmission electron microscopy (HR-TEM, JEM 2100F, JEOL, Japan). Thermogravimetric analysis (TGA) was carried out using a TA Instruments Q50 thermal analyzer under a nitrogen flow rate of 30 mL min^{-1} and a heating rate of 10°C min^{-1}.

The mechanical properties of the nanocomposites were measured at an elongation rate of 10 mm min^{-1} at room temperature using a tensile tester machine (Instron 4468). The shape memory properties were evaluated by elongating the specimens by 200% at 45°C and maintaining them at that temperature for 10 min. The samples were then quenched at 0 to 5°C and kept at that temperature for 10 min after removing the applied force. Finally, samples were heated to 60°C and kept there for 10 min, while the shape change of the samples during heating was recorded using a digital camera. Thermoresponsive shape recovery was calculated using the following equations:

$$\text{Shape retention} = (L_1 - L_0)/L_0 \times 100 \quad (1)$$

$$\text{Shape recovery} = (2L_0 - L_2)/L_0 \times 100 \quad (2)$$

where L_0, L_1, and L_2 are the initial, deformed, and final lengths of the samples.

The photothermal shape memory properties of the composites were measured by exposing the samples to a near-infrared (NIR) laser with a wavelength of 808 nm and a power of 70 mW/cm^2, following previously established parameters.[35] The samples were elongated by 100% at 45°C and kept at that temperature for 10 min. They were then quenched at 0 to 5°C and kept at that temperature for 10 min after the applied force was removed. Photothermal shape recovery was obtained by irradiating a shape fixed sample with the NIR laser, where the position of the laser beam was moved from one end to the other end of the sample at a constant speed of approximately 7.5 cm min^{-1}. The temperature of the samples was monitored with an infrared camera (Thermovision A320 M, FLIR Systems).

RESULTS AND DISCUSSION

Modified graphene holds significant potential for use in new materials, such as polymer nanocomposites. In this case, controlling interfacial interactions between the filler and the polymer is crucial in modulating polymer properties. Functionalization, which can directly control these interactions, is therefore particularly important. Meanwhile, Cu(I)-catalyzed Huisgen 1,3-dipolar cycloaddition between azides and alkynes has proven to be a particularly important reaction within click chemistry, and has been used in the design and synthesis of a wide range of functional materials.

The strategy we employ is useful in that this reaction proceeds with high efficiency and the excellent tolerance of many other functional groups. In addition, the triazole linkages that result are highly stable to hydrolysis, oxidation, and reduction. Furthermore, the chemical structure, molecular weight, and polydispersity index of presynthesized polymers used in the click reaction are known. Finally, grafting from approach shows good controllability of the grafted polymer content as well as high and even grafting efficiency.

The covalently functionalized hyperbranched polyurethane-grafted nanocomposites in this study were prepared by click coupling between HPU-alkyne and GO-Azide; the synthetic strategy is outlined in Scheme 1. The alkyne group density was modulated by incorporation of the alkyne-functionalized triol propargyl pentaerythritol into the feed of the reaction. The azide group was introduced to the graphene surface by subsequent treatment with 2-chloroisocyanate and sodium azide.

The GO-Azide surface functional groups were analyzed by FT-IR spectroscopy [Figure 1(a)]. A characteristic azide peak was observed at 2117 cm^{-1}, confirming successful surface modification. XPS was also used to analyze surface functionalization; the wide scan spectra of GO and GO-Azide are displayed in Figure 1(b). Signals at about 285.0 (C1s) and 532.0 eV (O1s) are clearly present for both samples. An additional peak at 399.5 eV (N1s) was observed for GO-Azide, further confirming azide integration. Meanwhile, the C1s spectrum of the GO starting material in Figure 2 shows the individual carbon bonds, with sp^2-hybridized aromatic carbon atoms (C═C, 284.4 eV), carbonyl carbon atoms (C═O, 287.8 eV) and carbon atoms bound to hydroxyl groups (C—O, 286.8 eV). Azide integration

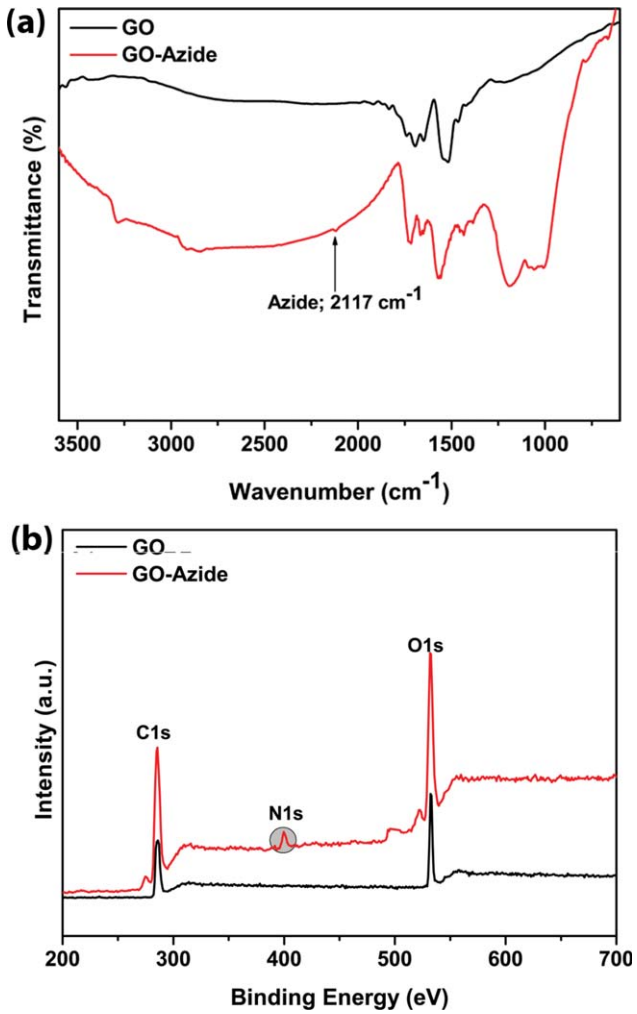

Figure 1. (a) FT-IR and (b) XPS spectra of GO and GO-azide. [Color figure can be viewed in the online issue, which is available at wileyonlinelibrary.com.]

decreased C—O intensity, which suggests a possible reaction between the hydroxyl and isocyanate groups.

Propargyl pentaerythritol was prepared following a previously established protocol[33,34] in which orthoacetate-protected pentaerythritol is first reacted with propargyl bromide and then deprotected to form the desired compound. Successful synthesis was confirmed by the presence of a characteristic IR peak at 2110 cm^{-1}.

The synthesis of hyperbranched polyurethane was carried out through an "$A_2 + B_3$" approach (Scheme 1), where the PCL-based, isocyanate terminated prepolymer and excess 4,4′-methylene *bis*(phenylisocyanate) served as the A_2 monomer and propargyl pentaerythritol served as the B_3 monomer. To avoid gel formation, the reaction was carried out in two steps process, where the first step was prepolymer synthesis and second step was branching formation.

The FT-IR spectra [Figure 3(a)] were obtained for structural analysis and to confirm completion of alkyne group pendent hyperbranched polyurethane. The –NCO absorption band at

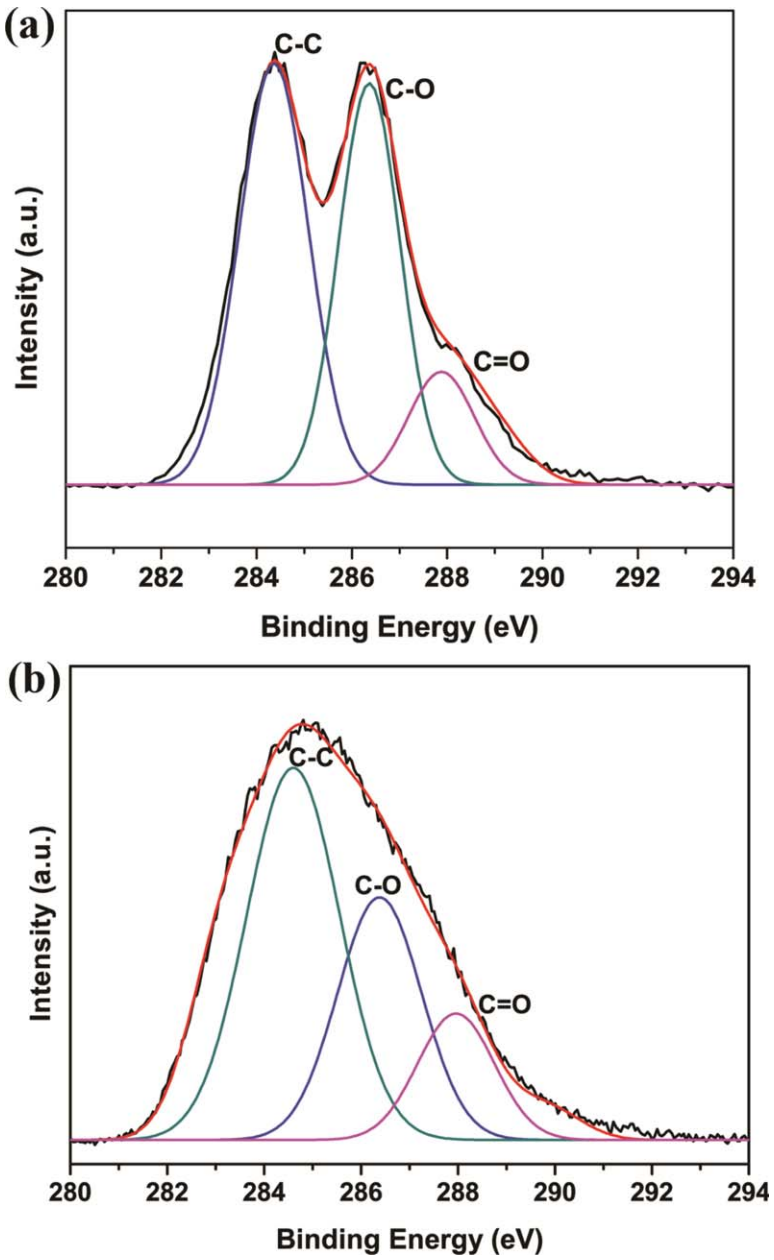

Figure 2. High-resolution C1s XPS spectra of (a) GO and (b) GO-azide. [Color figure can be viewed in the online issue, which is available at wileyonlinelibrary.com.]

2250 to 2270 cm^{-1} disappeared, confirming successful completion of the reaction. The peaks at 1651 and 1724 cm^{-1} correspond to C═C and ester stretching, respectively, while the peaks at 2932 and 2864 cm^{-1} are due to aliphatic -C-H symmetric and asymmetric stretching, respectively. In addition, the peaks at 1505 to 1580 cm^{-1} are the result of -N-H stretching.[3] The ^1H NMR spectra [Figure 3(b)] also confirmed HPU-alkyne formation, with -NH urethane linkage protons at 9.6 to 9.4 ppm, aliphatic $–CH_2$ protons at 5.1 to 1.2 ppm, with the wide range being due to their different chemical environments, and alkyne –CH protons at 2.1 ppm. The aromatic MDI protons appeared at 7.33 to 7.01 ppm as a multiplet.[3]

The click reaction was performed at 60°C using a CuBr/PMDETA catalyst in DMF for 24 h under continuous nitrogen flow (Scheme 1). FT-IR measurements were performed to allow for a better understanding of the chemical transformation of HPU-alkyne after click coupling with GO-Azide. The alkyne peak vanished after the reaction was complete, indicating successful synthesis.

The degree of GO-grafting was determined by isolating the pure polymer (HPU) from the hyperbranched polyurethane-*grafted*-GO (HPU-*g*-GO). A pure powder of the product from GHPU was obtained by sequential redissolving, sonication, and

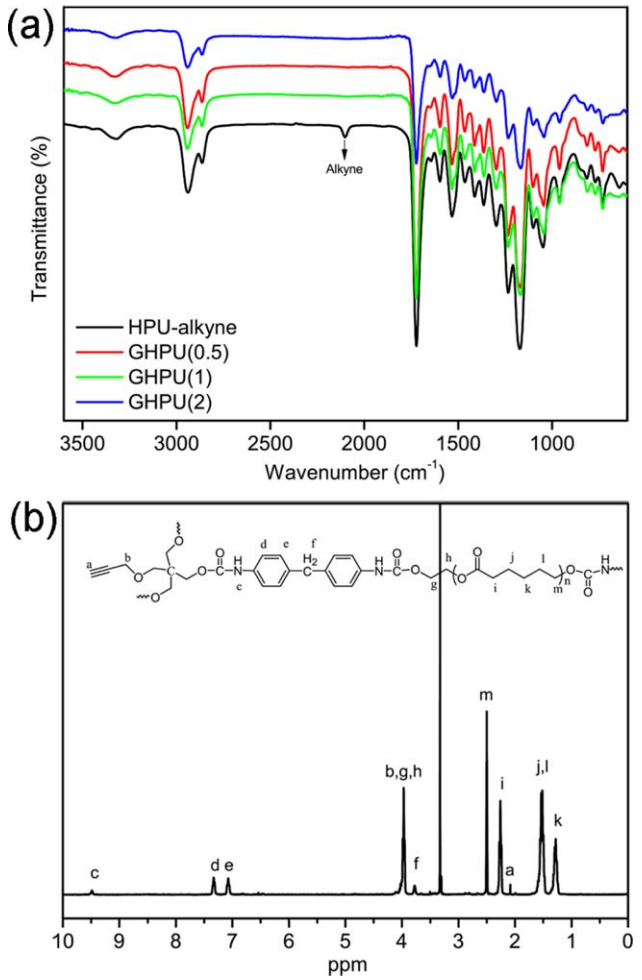

Figure 3. (a) FT-IR of HPU-alkyne and GHPU samples, and (b) ^{1}H NMR spectra of GHPU (1). [Color figure can be viewed in the online issue, which is available at wileyonlinelibrary.com.]

centrifugation with DMF and the samples are denoted as HPU-*g*-GO(0.5), HPU-*g*-GO(1), and HPU-*g*-GO(2), respectively. The DMF solution of HPU-*g*-GO showed superior dispersion and stability after sonication when compared with pure GO, even after 1 week. This may be due to the click grafting of hyperbranched polymer on GO surface, which facilitates greater stability and solubility in an organic solvent (Figure 4).

TEM confirmed that GO forms individual sheets in DMF as a result of ultrasonic treatment [Figure 5(a)]. Meanwhile, the HPU-*g*-GO graphene surfaces were covered by black patches, which likely correspond to the grafted polymer [Figure 5(b–d)]. In addition, the increased steric bulk of the sheets as a result of grafting clearly prevented any aggregation. The high level of graphene dispersion observed directly correlated with improved physical and thermal properties.

The crystallization and melting behaviors are the key factors for shape memory polymers such as segmented polyurethane. Figure 6 shows the DSC curves measured during cooling and its reheating of the pure HPU and the nanocomposites. All samples show an exothermic peak and endothermic peak, which can be attributed to the crystallization and melting of the soft-segment phase, respectively. Graphene incorporation increased the crystallization temperature for all composites, with the effect being more significant for the sample containing 2.0 wt % GO. This implies that GO incorporation aided heterogeneous nucleation. Thus, the increase in crystallization temperature of the PCL soft segment indicates a good chemical affinity and interaction between the nanofillers and HPU due to covalent bonding via click coupling.[36] Enhanced soft-segment crystallinity of HPU/GO nanocomposites increases the storage capacity of strain-induced energy for thermal-triggered shape recovery. Furthermore, the melting temperature of the nanocomposites is higher than that of the pure HPU, which suggests more oriented polymer chains and a better defined crystal structure.

TGA curves of click coupled nanocomposites with different amount of GO are shown in Figure 7(a). HPU undergoes a two-step degradation, resulting from sequential loss of the soft and hard segments of polyurethane. From Figure 7(a), it is noticeable that the thermal stability is significantly enhanced for nanocomposites with an increased GO loading, as compared with pure HPU. On loading of 2.0 wt % GO, the thermal stability at 90 wt % of the GHPU(2) nanocomposites increased, compared with that of HPU from 260 to 300°C (increased by about 40°C), indicating that the thermal stability of polyurethane is enhanced by functionalization with graphene sheets. This improved stability likely results from the fact that the distributed graphene sheets can act as barriers, as per the tortuous path model, to prevent the permeation of oxygen, the liberation of volatile degradation products, and the formation of char.[37,38] The GO surface may also act as a radical scavenger, deferring the onset of thermal degradation.

Good dispersion of the reinforcing fillers in polymer composites ensures maximized strengthened surface area. This affects the neighboring polymer chains, in turn spreading throughout the entire composite. In order to prepare high-performance graphene polymer composites, well dispersed and high-surface nanofiller is not enough; another crucial key is to strengthen the interfacial adhesion in order to achieve efficient load transfer between the graphene sheets and the polymer matrix. Hence, uniformly dispersed HPU-*g*-GO should have a momentous impact on the host matrix.

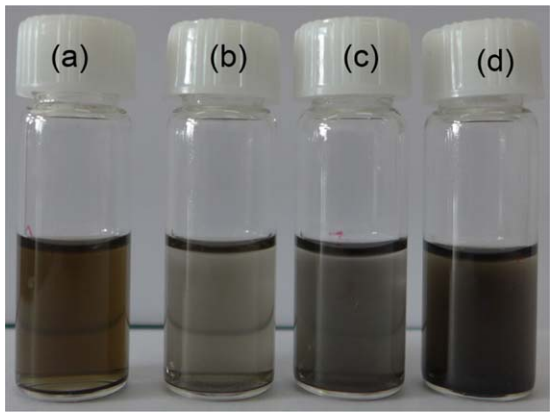

Figure 4. Solubility in DMF of (a) GO, (b) HPU-*g*-GO(0.5), (c) HPU-*g*-GO(1), and (d) HPU-*g*-GO(2). [Color figure can be viewed in the online issue, which is available at wileyonlinelibrary.com.]

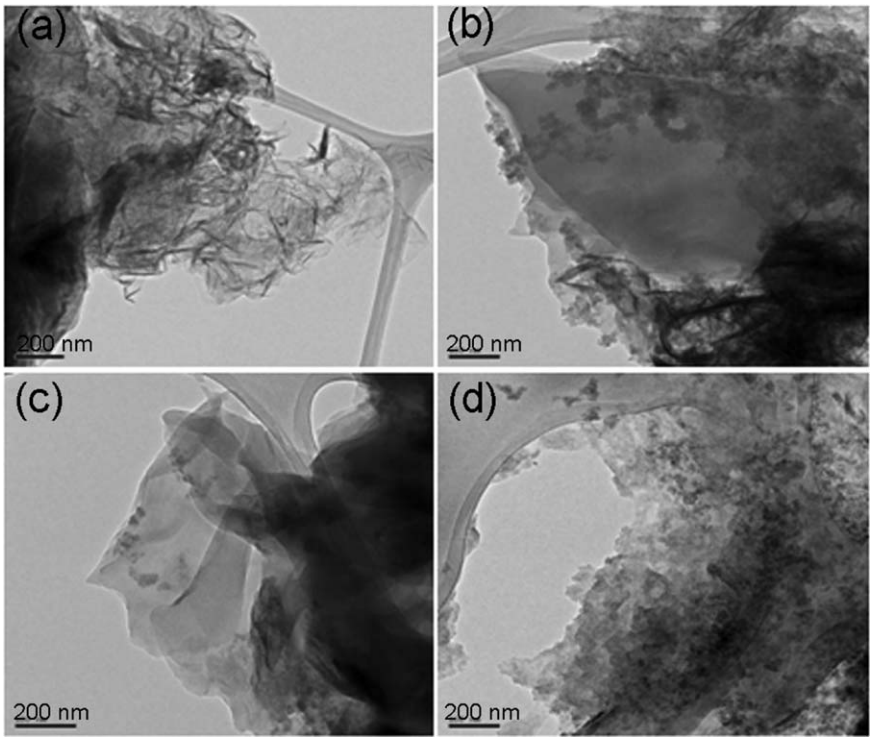

Figure 5. Grafting of HPU onto GO as shown in the TEM images of (a) GO (b) HPU-*g*-GO(0.5), (c) HPU-*g*-GO(1), and (d) HPU-*g*-GO(2).

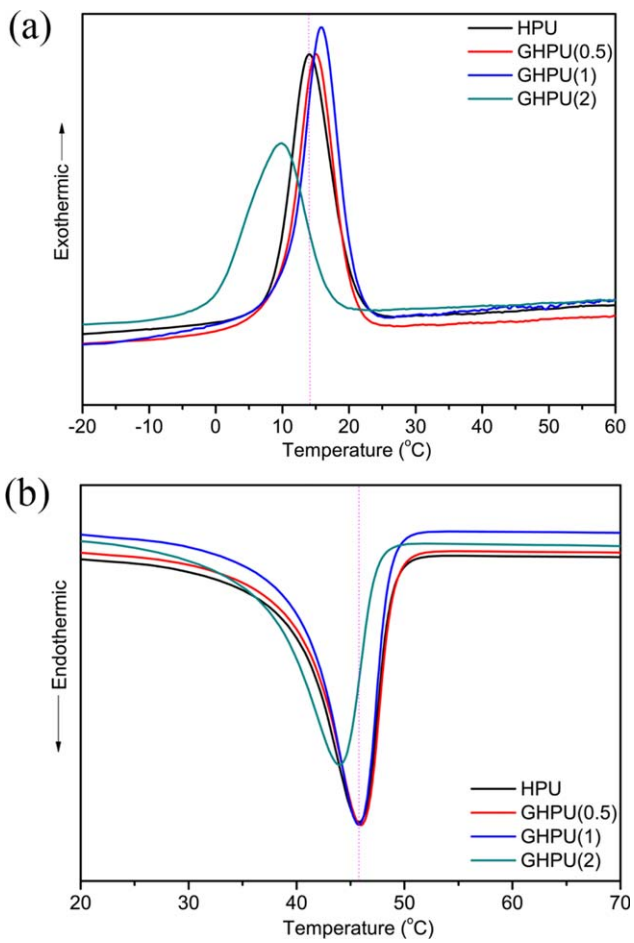

Figure 6. DSC thermograms measured during (a) cooling from the melting temperature and (b) the second heating of the pure HPU and GHPU nanocomposites. [Color figure can be viewed in the online issue, which is available at wileyonlinelibrary.com.]

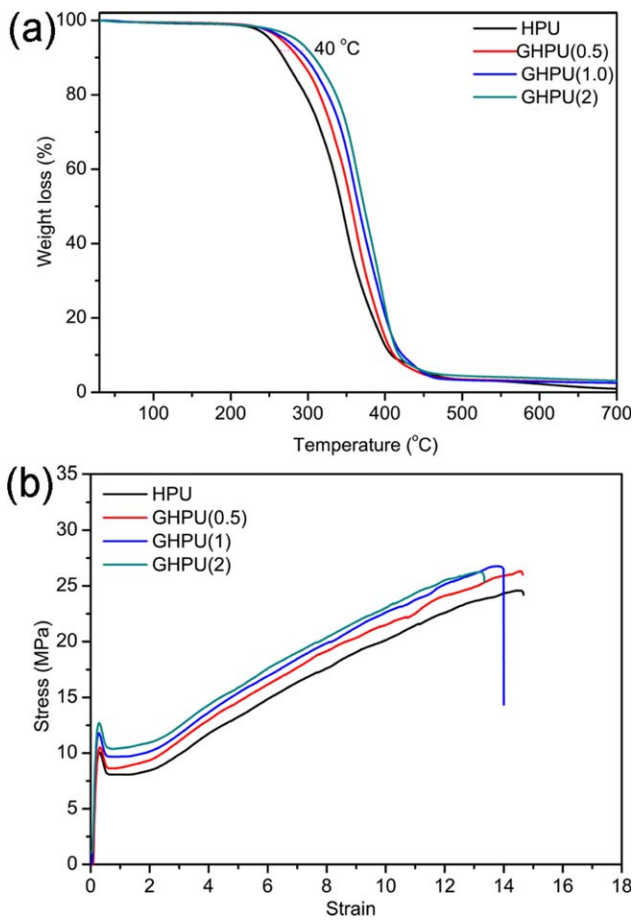

Figure 7. (a) TGA analysis and (b) stress–strain curves of pure HPU and GHPU films. [Color figure can be viewed in the online issue, which is available at wileyonlinelibrary.com.]

Table I. Mechanical and Thermoresponsive Shape Memory Properties of the Pure HPU and GHPU Nanocomposite Films

Properties	HPU	GHPU (0.5)	GHPU (1)	GHPU (2)
Breaking stress (MPa)	24.1	26.3	26.8	26.1
Strain	14.5	14.6	13.9	13.2
Modulus (MPa)	78.2	101.6	118.3	126.8
Shape retention (%)	84	87	90	94
Shape recovery (%)	90	94	97	98

Figure 7(b) shows the stress-strain curves for pure HPU and GHPU nanocomposites at different loadings, while the Young's modulus, breaking stress, and strain-at-break are summarized in Table I. The modulus increased with graphene content, with a 64% increase from pure HPU for the 1 wt % GO sample. Samples incorporating up to 1 wt % GO also showed excellent strength and stretchability, as evidenced by the very high breaking stress and elongation-at-break. In this case, the HPU chains and the free functional groups on the basal plane or edge on the surface of HPU-*g*-GO may provide a stronger interaction and interlocking in the HPU matrix. This results in more effective load transfer and a significant increase in mechanical properties.

Thermoresponsive shape memory properties for the nanocomposites samples are also provided in Table I. The GHPU nanocomposites displayed better thermoresponsive shape memory performance than pure HPU. Good dispersion and high nanofiller compatibility help here as well, yielding higher shape recovery due to the release of stored elastic strain energy. As the SMPs can go through two phases above and below this transition temperature, the mechanical energy applied on the material during deformation is accumulated. In turn, reestablishing network chain conformational entropy forces the material back to its original form. GHPU(2) nanocomposites showed the best properties out of all the samples, which is consistent with the fact that increased loading would increase this effect. These click coupled GO shape memory nanocomposites may have good advantages in thermoresponsive and photothermal shape recovery actuation due to the enhanced GO dispersion and relatively less surface defects in GO functionalization, compared with the shape memory nanocomposites with pure GO and functionalized GO using no click reaction.[39–41]

Photothermal shape recovery was also studied for the GHPU films using an NIR laser. The unusual photothermal properties of these kinds of nanocomposites arise from the localized surface plasmon resonance of the graphene sheets.[35] Figure 8(a) demonstrates that samples with a higher GO content undergo a greater increase in temperature due to NIR irradiation. Meanwhile, photothermal shape recovery of the nanocomposite films is shown in Figure 8(b), for which samples were irradiated along a longitudinal direction after elongation by 100% at 60°C and quenching in ice water for shape fixation. Light from the laser is absorbed by the graphene in the samples and converted to thermal energy to actuate the nanocomposites. Photothermal shape recovery values of 93.5, 93.8, and 96.2% were obtained for GHPU(0.5), GHPU(1), and GHPU(2), respectively, indicating that the nanocomposites hold potential for thermoresponsive and

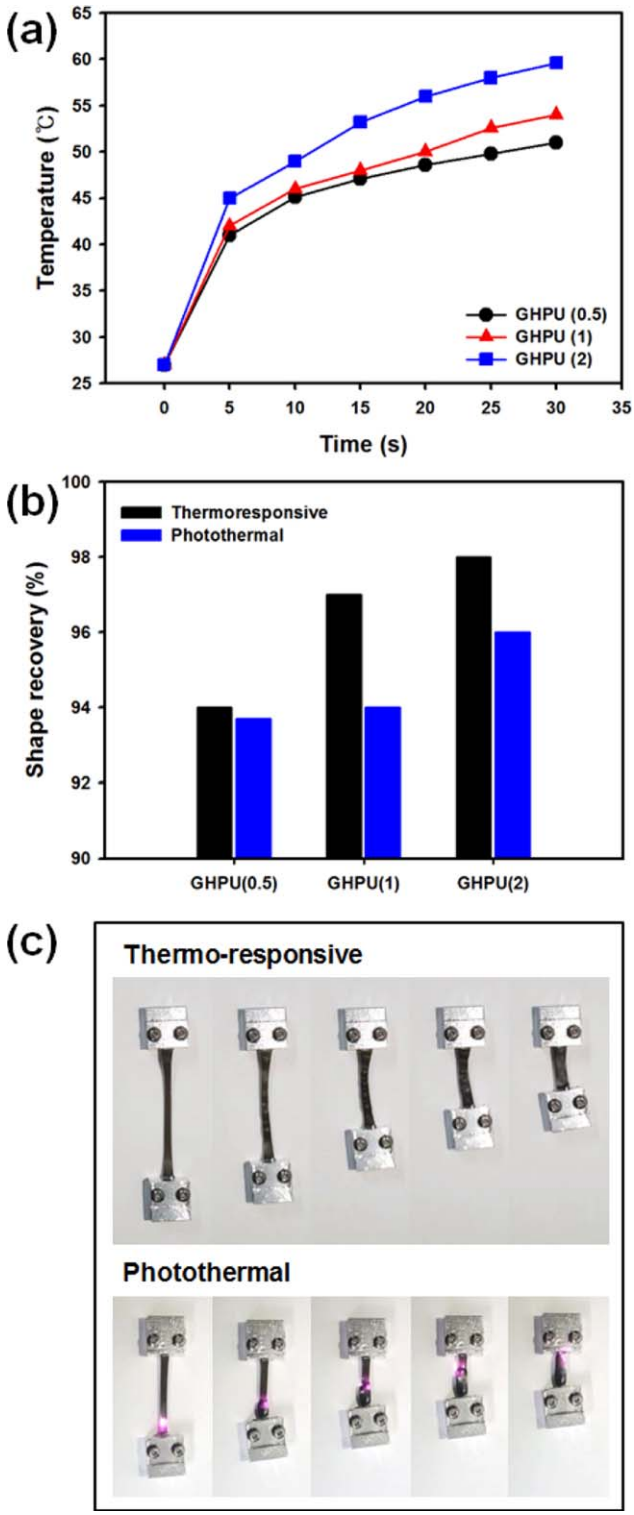

Figure 8. (a) The photothermal heating curves, (b) thermoresponsive and photothermal shape recovery of the GHPU films, and (c) photo images for shape recovery of GHPU(1). [Color figure can be viewed in the online issue, which is available at wileyonlinelibrary.com.]

photothermal shape memory applications. The thermoresponsive and photothermal shape recovery actuation of the GHPU(1) is demonstrated in Figure 8(c).

CONCLUSIONS

We demonstrated a novel approach to the fabrication of high performance polymer nanocomposites in which the GO sheets were covalently functionalized via click coupling with a HPU matrix. The mechanical, thermal, and thermoresponsive and photothermal shape memory properties of the nanocomposites were enhanced due to good dispersion and interaction between the two phases. Results suggest that these nanocomposites could be used in potential shape memory applications.

ACKNOWLEDGMENTS

This article was supported by Konkuk University in 2014.

REFERENCES

1. Lendlein, A.; Kelch, S. *Angew. Chem. Int. Ed.* **2002**, *41*, 2034.
2. Meng, Y.; Jiang, J.; Anthamatten, M. *ACS Macro. Lett.* **2015**, *4*, 115.
3. Mahapatra, S. S.; Yadav, S. K.; Yoo, H. J.; Cho, J. W. *J. Mater. Chem.* **2011**, *21*, 7686.
4. Yu, K.; Liu, Y.; Leng, J. *RSC Adv.* **2014**, *4*, 2961.
5. Jung, Y. C.; Yoo, H. J.; Kim, Y. A.; Cho, J. W.; Endo, M. *Carbon* **2010**, *48*, 1598.
6. Jung, Y. C.; Kim, H. H.; Kim, Y. A.; Kim, J. H.; Cho, J. W.; Endo, M.; Dresselhaus, M. S. *Macromolecules* **2010**, *43*, 6106.
7. Lee, C. G.; Wei, X. D.; Kysar, J. W.; Hone, J. *Science* **2008**, *321*, 385.
8. Park, S.; Ruoff, R. S. *Nat. Nanotechnol.* **2009**, *4*, 217.
9. Geim, A. K. *Science* **2009**, *324*, 1530.
10. Rao, C. N. R.; Sood, A. K.; Subrahmanyam, K. S.; Govindaraj, A. *Angew. Chem. Int. Ed.* **2009**, *48*, 7752.
11. Cai, D. Y.; Song, M. *Mater. Chem.* **2010**, *20*, 7906.
12. Kuilla, T.; Bhadra, S.; Yao, D.; Kim, N. H.; Bose, S.; Lee, J. H. *Prog. Polym. Sci.* **2010**, *35*, 1350.
13. Li, X. L.; Wang, X. R.; Zhang, L.; Lee, S. W.; Dai, H. *J. Science* **2008**, *319*, 1229.
14. Stankovich, S.; Dikin, D. A.; Dommett, G. H. B.; Kohlhaas, K. M.; Zimney, E. J.; Stach, E. A.; Piner, R. D.; Nguyen, S. T.; Ruoff, R. S. *Nature* **2006**, *442*, 282.
15. Stankovich, S.; Dikin, D. A.; Piner, R. D.; Kohlhaas, K. A.; Kleinhammes, A.; Jia, Y.; Wu, Y.; Nguyen, S. T.; Ruoff, R. S. *Carbon* **2007**, *45*, 1558.
16. Bae, C. Y.; Park, J. H.; Kim, E. Y.; Kang, Y. S.; Kim, B. K. *J. Mater. Chem.* **2011**, *21*, 11288.
17. Park, S. J.; Dikin, D. A.; Nguyen, S. T.; Ruoff, R. S. *J. Phys. Chem. C* **2009**, *113*, 15801.
18. Mahapatra, S. S.; Karak, N. *J. Appl. Polym. Sci.* **2007**, *106*, 95.
19. Zhou, Y.; Huang, W.; Liu, J.; Zhu, X.; Yan, D. *Adv. Mater.* **2010**, *22*, 4567.
20. Gao, C.; Yan, D. *Prog. Polym. Sci.* **2004**, *29*, 183.
21. Voit, B. L.; Lederer, A. *Chem. Rev.* **2009**, *109*, 5924.
22. Thakur, S.; Karak, N. *RSC Adv.* **2013**, *3*, 9476.
23. Salavagione, H. J.; Gomez, M. A.; Martinez, G. *Macromolecules* **2009**, *42*, 6331.
24. Fang, M.; Wang, G.; Lu, H. B.; Yang, Y. L.; Nutt, S. *J. Mater. Chem.* **2009**, *19*, 7098.
25. Rostovtsev, V. V.; Green, L. G.; Fokin, V. V.; Sharpless, K. B. *Angew. Chem. Int. Ed.* **2002**, *41*, 2596.
26. Tornoe, C. W.; Christensen, C.; Meldal, M. *J. Org. Chem.* **2002**, *67*, 3057.
27. Li, H. M.; Cheng, F. O.; Duft, A. M.; Adronov, A. *J. Am Chem. Soc.* **2005**, *127*, 14518.
28. Yadav, S. K.; Mahapatra, S. S.; Cho, J. W. *Polymer* **2012**, *53*, 2023.
29. He, H. K.; Zhang, Y.; Gao, C.; Wu, J. Y. *Chem. Commun.* **2009**, 1655.
30. Zhang, Y.; He, H. K.; Gao, C. *Macromolecules* **2008**, *41*, 9581.
31. Zhang, W. B.; Tu, Y.; Ranjan, R.; Van Horn, R. M.; Leng, S.; Wang, J.; Polce, M. J.; Wesdemiotis, C.; Quirk, R. P.; Newkome, G. R.; Cheng, S. Z. D. *Macromolecules* **2008**, *41*, 515.
32. Stankovich, S.; Piner, R. D.; Nguyen, S. T.; Ruoff, R. S. *Carbon* **2006**, *44*, 3342.
33. Burai, R.; Chatwichien, J.; McNaughton, B. R. *Org. Biomol. Chem.* **2011**, *9*, 5056.
34. Gorodetskaya, I. A.; Choi, T. L.; Grubbs, R. H. *J. Am. Chem. Soc.* **2007**, *129*, 12672.
35. Yi, D. H.; Yoo, H. Y.; Mahapatra, S. S.; Kim, Y. A.; Cho, J. W. *J. Colloid Interface Sci.* **2014**, *432*, 128.
36. Feng, Y.; Qin, M.; Guo, H.; Yoshino, K.; Feng, W. *ACS Appl. Mater. Interfaces* **2013**, *5*, 10882.
37. Cao, Y. W.; Lai, Z. L.; Feng, J. C.; Wu, P. Y. *J. Mater. Chem.* **2011**, *21*, 9271.
38. Cai, D. Y.; Song, M. *J. Mater. Chem.* **2010**, *20*, 7906.
39. Yi, D. H.; Yoo, H. J.; Cho, J. W. *Fibers Polym.* **2015**, *16*, 1766.
40. Yadav, S. K.; Cho, J. W. *Appl. Surf. Sci.* **2013**, *266*, 360.
41. Choi, J. T.; Dao, T. D.; Oh, K. M.; Lee, H. I.; Jeong, H. M.; Kim, B. K. *Smart Mater. Struct.* **2012**, *21*, 075017.